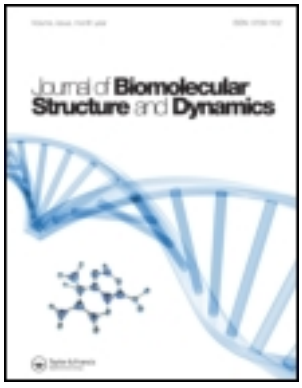

Journal of Biomolecular Structure and Dynamics
Publication details, including instructions for authors and subscription information:
http://www.tandfonline.com/loi/tbsd20

Inhibition of mushroom tyrosinase by a newly synthesized ligand: inhibition kinetics and computational simulations

Mahdi Alijanianzadeh [a], Ali Akbar Saboury [a], Mohammad Reza Ganjali [b], Hamid Hadi-Alijanvand [a] & Ali Akbar Moosavi-Movahedi [a]

[a] Institute of Biochemistry and Biophysics, University of Tehran, Tehran, Iran

[b] Center of Excellence in Electrochemistry, Faculty of Chemistry, University of Tehran, Tehran, Iran

Version of record first published: 11 Jun 2012.

To cite this article: Mahdi Alijanianzadeh, Ali Akbar Saboury, Mohammad Reza Ganjali, Hamid Hadi-Alijanvand & Ali Akbar Moosavi-Movahedi (2012): Inhibition of mushroom tyrosinase by a newly synthesized ligand: inhibition kinetics and computational simulations, Journal of Biomolecular Structure and Dynamics, 30:4, 448-459

To link to this article: http://dx.doi.org/10.1080/07391102.2012.682210

Journal of Biomolecular Structure and Dynamics
Vol. 30, No. 4, 2012, 448–459

Inhibition of mushroom tyrosinase by a newly synthesized ligand: inhibition kinetics and computational simulations

Mahdi Alijanianzadeh[a], Ali Akbar Saboury[a]*, Mohammad Reza Ganjali[b], Hamid Hadi-Alijanvand[a] and Ali Akbar Moosavi-Movahedi[a]

[a]*Institute of Biochemistry and Biophysics, University of Tehran, Tehran, Iran;* [b]*Center of Excellence in Electrochemistry, Faculty of Chemistry, University of Tehran, Tehran, Iran*

Communicated by Ramaswamy H. Sarma

(*Received 25 November 2011; final version received 2 March 2012*)

Alterations in the synthesis of melanin contribute to a number of diseases; therefore, the design of new tyrosinase inhibitors is very important. Mushroom tyrosinase (MT) is a metalloenzyme, which plays an important role in melanin biosynthesis. In this study, the inhibitory effect of a novel designed compound, i.e. 2-((1Z)-(2-(2,4-dinitrophenyl)hydrazin-1-ylidene)methyl) phenol, as a specific ligand which can bind to the copper ion of MT, has been assessed. The ligand was found to competitively inhibit both the cresolase and catecholase activities of MT, with small inhibition constants of 2.8 and 2.6 μM, respectively. Intrinsic fluorescence studies were performed to gain more information on the binding constants. Docking results indicated that the ligand binds to copper ions in the active site of MT via the OH group of the ligand. The ligand makes four hydrogen bonds with aspartic acid and one hydrogen bond with the histidine residue in the active site. Molecular dynamics results show that ligand binds to the MT via both electrostatic and hydrophobic interactions with its different parts.

Keywords: mushroom tyrosinase; inhibition; cresolase; catecholase

Introduction

Tyrosinase (EC 1.14.18.1) is a copper-containing enzyme that is widely distributed in microorganisms, animals, and plants (Robb, 1984; Whitaker, 1995; Zawistowski, 1991). The enzyme catalyzes both the cresolase activity (monophenolase activity) that hydroxylates monophenol (L-tyrosine) to diphenol (L-Dopa) and the catecholase activity (diphenolase activity) that oxidizes diphenol (L-Dopa) to *o*-quinone (Sanchez-Ferrer, Rodriguez-Lopez, Garcia-Canovas, & Garcia-Carmona, 1995). Tyrosinase is responsible for skin pigmentation (Cho et al., 2009).

The enzymatic oxidation of L-tyrosine to melanin is very important because melanin has many functions, and alterations in the synthesis of melanin contribute to some diseases (Prezioso, Epperly, Wang, & Bloomer, 1992). Finding new tyrosinase inhibitors with low K_i values is very important, because the enzyme has a major role in both mammalian melanogenesis and enzymatic browning of fruits or fungi.

In melanogenesis, some pigments, like melanin, are produced through the combination of enzymatically catalyzed and chemical reactions. Raper (1928) and Mason (1948) elucidated the biosynthetic pathway of the formation of melanin, and Cooksey et al. (1997) and Schallreuter, Kothari, Chavan, & Spencer (2008) modified this pathway.

During melanogenesis, firstly tyrosinase oxidizes tyrosine to dopaquinone, which is the rate-determining step because the remainder of the reaction sequence can spontaneously proceed at the physiological pH values (Halaban et al., 2002). Melanin protects human skin from the harmful effects of UV from the sun (Artés & Gil, 1998). Since hyperpigmentation in human skin is not desirable, researchers are interested in finding new potent tyrosinase inhibitors for the use in anti-browning and skin whitening.

The active site of tyrosinase has a di-copper center that is similar but not identical to hemocyanins (Eicken, Krebs, & Sacchettini, 1999; Orlow et al., 1994). Each copper ion in the active site is coordinated by three nitrogen atoms from the three adjacent histidine residues (Cooksey, Garratt, Land, Ramsden, & Riley, 1998; Rescigno, Sollai, Pisu, Rinaldi, & Sanjust, 2002). Mushroom tyrosinase (MT) is the commercially available tyrosinase.

*Corresponding author. Email: saboury@ut.ac.ir

ISSN 0739-1102 print/ISSN 1538-0254 online

http://dx.doi.org/10.1080/07391102.2012.682210
http://www.tandfonline.com

The control of tyrosinase activity has been of special interest among investigators due to its potential use in medicinal, cosmetic, and agricultural products (Parvez, Kang, Chung, & Bae, 2007). Therefore, understanding the catalysis mechanism of tyrosinase and its regulation, including its inhibition, is important. To understand the mechanism of the enzymatic and inhibition reactions, many studies have been performed to obtain additional information about the function of MT (Gheibi, Saboury, Haghbeen, & Moosavi-Movahedi, 2005; Haghbeen, Saboury, & Karbassi, 2004; Karbassi, Saboury, Ranjbar, & Moosavi-Movahedi, 2003; Parvez et al., 2007; Saboury et al., 2004; Shareefi Borojerdi, Haghbeen, Asghar Karkhane, Fazli, & Saboury, 2004).

After introducing two new bi-pyridine synthetic compounds as potent uncompetitive MT inhibitors (Saboury et al., 2004), the inhibitory effects of three synthetic n-alkyl dithiocarbamates (Gheibi, Saboury, Mansuri-Torshizi, Haghbeen, & Moosavi-Movahedi, 2005), *n*-alkyl xanthates (Alijanianzadeh, Saboury, Mansuri-Torshizi, Haghbeen, & Moosavi-Movahedi, 2007; Saboury & Alijanianzadeh, 2008; Saboury, Alijanianzadeh, & Mansoori-Torshizi, 2007), and benzyl and *p*-xylidine-bisdithiocarbamate (Amin, Saboury, Mansuri-Torshizi, & Moosavi-Movahedi, 2010) were elucidated. Also recently, the inhibitory effects of isophthalic acid, dithioglycerine, Cl^-, and thiobarbituric acid on MT have been studied (Han et al., 2007; Park, Lyou, Hahn, Hahn, & Yang, 2006; Si et al., 2011; Yin et al., 2011). We hypothesized that the ligand's hydroxyl group may block MT activity by binding to tyrosinase's Cu atoms in the active site based on the fact that previous findings had shown the role of hydroxyl groups in tyrosinase inhibition (Arung, Shimizu, & Kondo, 2006; Fu, Li, Wang, Lee, & Cui, 2005; Gao, Nishida, Saito, & Kawabata, 2007; Hyun, Lee, Jeong da, Kim, & Choi, 2008; Jeong et al., 2009; Kanade, Suhas, Chandra, & Gowda, 2007; Kim et al., 2006; Kim, Son, Chang, Kang, & Kim, 2003; Kubo et al., 2000; Kubo & Kinst-Hori, 1999; Lee et al., 2002; Shiino, Watanabe, & Umezawa, 2001, 2003; Shimizu, Kondo, & Sakai, 2000; Shin et al., 1998; Yamazaki, Kawano, Yamanaka, & Maruyama, 2009; Yan et al., 2009; Yokota, Nishio, Kubota, & Mizoguchi, 1998).

Currently, there is a great deal of interest in drug design investigations involving ligand and protein interactions and different theoretical methodologies have been applied to the drug design in a variety of biological systems and there have been extensive publications in this journal (Banappagari, Ronald, & Satyanarayanajois, 2010; Cambria, Di Marino, Falconi, Garavaglia, & Cambria, 2010; Chang et al., 2010; da Cunha, Barbosa, Oliveira, & Ramalho, 2010; Huang et al., 2010; Kahlon, Roy, & Sharma, 2010; Nasiri, Bahrami, Zahedi, Moosavi-Movahedi, & Sattarahmady, 2010; Nekrasov & Zinchenko, 2010; Ompraba, Velmurugan, Louis, & Rafi, 2010; Ramalho, Rocha, da Cunha, Oliveira, & Carvalho, 2010; Tao, Rao, & Liu, 2010; Yang et al., 2010).

Due to our interest in designing an inhibitor for tyrosinase, we expected that by blocking the Cu^{+2} in the active site, the enzyme activity would be inhibited. Recently, the three-dimensional structure of MT has been determined (Ismaya, Rozeboom, Schurink et al., 2011; Ismaya, Rozeboom, Weijn et al., 2011). For gaining more insights into the binding model, a docking study was also performed in this study and the inhibitory effect of the newly synthesized ligand was examined besides evaluating kinetics analysis of it in both cresolase and catecholase activities.

Materials and methods

MT (MT; EC 1.14.18.1), specific activity 5340 units/mg, L-Dopa, and L-tyrosine were purchased from Sigma Co. (Madrid, Spain) 2-((1Z)-(2-(2,4-dinitrophenyl)hydrazin-1-ylidene)methyl)phenol was synthesized as described below (Figure 1). ^{1}H NMR spectra were recorded using a Brucker DRX-500 Avance Spectrophotometer at 500 MHz in DMSO-d_6 and $CDCl_3$ using TMS as internal reference. ^{1}H NMR data are expressed in parts per million (ppm) and are reported as chemical shift position (δH), multiplicity (s = singlet, d = doublet, t = triplet, q = quartet, m = multiple), and assignment. A phosphate buffer (10 mM, pH 6.8) was used throughout this research and the corresponding salts were obtained from Merck Co. All experiments were carried out at 20°C. Ultrapure water was used throughout this research.

Synthesis of the ligand

2,4-Dinitro phenyl hydrazine (.01 mol), salicylaldehyde (.01 mol), and a catalytic amount of toluene-4-sulfonic

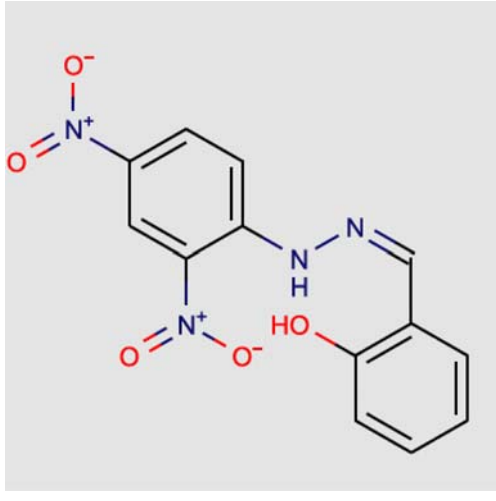

Figure 1. The chemical structure of 2-((1Z)-(2-(2,4-dinitrophenyl)hydrazin-1-ylidene)methyl)phenol as the newly synthesized ligand.

acid were refluxed in benzene (50 mL) for 5.5 h. Then the solvent was evaporated to 20 mL to obtain the red crystals of the product with a yield of 90%. ^{1}H NMR (500 MHz, DMSO-d_6, ppm): δH = 5.53 (1H, s, OH), 7.18–7.98 (9H, m, H_{Ar}), 8.79 (1H, s, = CH), and 12.31 (1H, s, NH).

Kinetic measurements

Catecholase and cresolase activities of MT were determined in the reaction medium for 1 and 2 min with enzyme concentrations of 11.11 and 112.68 μg/ml by spectrophotometrically measuring the rate of dopachrome formation at 475 nm ($\varepsilon = 3700\ M^{-1}\ cm^{-1}$) in the first two minutes, using a Cary spectrophotometer, 100 Biomodel, with jacketed cell holders (Cabanes, Garcia-Canovas, Lozano, & Garcia-Carmona, 1987). The assay was performed with slight modifications as previously described (Chen & Kubo, 2002). Freshly dissolved enzyme, substrate, and ligand were used in this work. All enzymatic reactions were performed in a phosphate buffer (10 mM) at pH 6.8 in a conventional thermostated quartz cell. Substrate addition followed after incubation of the enzyme with different concentrations of the ligand. The initial rate was measured in each assay and all assays were repeated three times.

Fluorescence quenching study

The fluorescence intensities were recorded using a Carry Eclipse Spectrofluorophotometer (Varian, Australia) at an excitation wavelength (λ_{ex}) of 290 nm. The maximum emission wavelength (λ_{em}) for the MT was 340 nm. MT (1 μM) was chosen as the concentration for the fluorescence-quenching experiments. Series of the ligand solutions with different concentrations of 2.7, 6, 7.5, 9.5, and 14 μM were prepared in the phosphate buffer.

According to a previous report (Xie, Xu, & Wang, 2005), when small molecules are bound to equivalent sites on a macromolecule, the equilibrium between free and bound molecules is given by Equation (1) to evaluate the binding constant (K) and number of binding sites (n):

$$F_0/(F_0F) = 1/n + 1/K \times 1/[Q] \quad (1)$$

where F_0 and F are the relative steady-state fluorescence intensities in the absence and presence of quencher, respectively. [Q] is the quencher (ligand) concentration and values for K and n can be derived from the intercept and slope of a plot based on the above equation.

In silico *docking of the tyrosinase structure and ligand and molecular dynamics simulation*

The minimized 3D structure of tyrosinase was the input structure of HEX 5.1 protein docking software as the receptor. A blind docking was run with a pre-generated ligand structure. The docking processes were performed under shape and electrostatic correlation types in HEX (Ritchie, 2003). A set of docking result was generated by HEX and the complex with the lowest energy was chosen as the best. The post-processing refinements were Newton-like minimizations based on optimized potentials for liquid simulations force field parameters. The final structure was saved as a pdb file. To study the dynamics of tyrosinase–ligand interaction, NAMD 2.8 engine was used (Phillips et al., 2005). Generalized born implicit solvent was used to reach an accurate and fast molecular dynamics (MD). Constant temperature (300 K) MD was performed by using langevin thermostat. Non-bonded interaction cutoff sets to 13.5 A. Integration time step sets to 2 fs. Before starting the production MD, protein–ligand system was minimized for 2 ps and final production run continued for 12 ns. To build the ligand CHARMM force field, starting parameters were obtained from ParamChem server before further routine justifications.

Results

The effect of the ligand on both activities of MT was examined at pH 6.8 and a temperature of 20°C. To assess the reversibility of the ligand-mediated inhibition, plots of the activity (catecholase activity) vs. the enzyme concentration ([E]) at different fixed concentrations of ligand were used (Figure 2). The results showed straight lines passing through the origin, indicating that the inhibition by ligand was reversible.

Kinetic parameters of cresolase activity of MT in the presence of ligand

The effect of the ligand on the cresolase activity of MT was examined and it was found to inhibit the cresolase

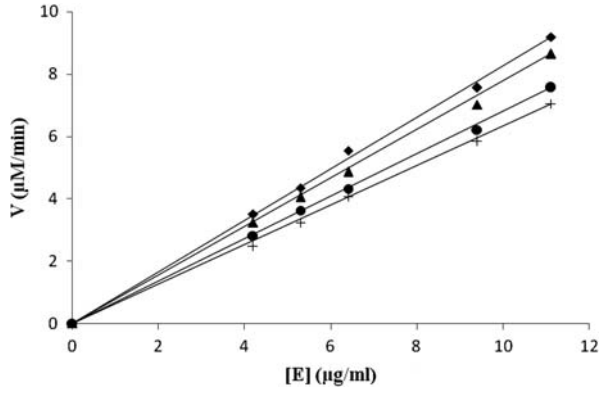

Figure 2. Plots of remaining activity, V (μM/min) (catecholase activity) vs. (E) (μg/ml). The ligand concentrations are 3 μM (◆), 4 μM (▲), 6 μM (●), and 7 μM (+). The final concentration of L-Dopa was 50 μM.

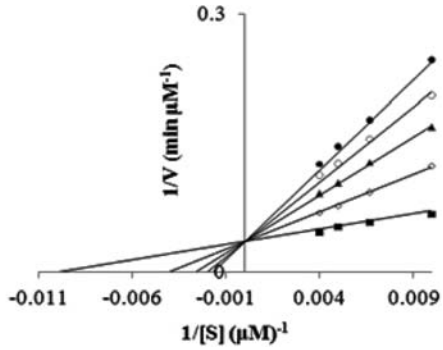

Figure 3. Double reciprocal Lineweaver–Burk plots of MT kinetic assay for cresolase reactions. L-tyrosine was a substrate. The reaction was done in 10 mM sodium phosphate buffer, pH 6.8, at 20°C and 112.68 μg/ml enzyme, in the presence of different concentrations of ligand,0 mM (■), 3 μM (◊), 7 μM (▲), 11 μM (◯), and 15 μM (●).

activity. Double reciprocal Lineweaver–Burk plot for the cresolase activity of MT assayed as hydroxylation of L-tyrosine in the presence of different fixed concentrations of ligand is shown in Figure 3. These plots show a set of straight lines, which intersect exactly on the vertical axis. As it is seen the value of maximum velocity (V_{max}) is unchanged by the inhibitor while the apparent Michaelis–Menten (K_m') values are increased, indicating that ligand induces a competitive inhibition. Figure 4 shows the secondary plot, the K_m' value at a given concentration of ligand vs. the concentration of inhibitor, which gives the inhibition constants (K_i) from the abscissa intercepts ($-K_i$). The K_i value for ligand is 2.8 μM, the small value of which shows that this ligand tightly binds to the enzyme.

Kinetic parameters of catecholase activity of MT in the presence of ligand

Double reciprocal Lineweaver–Burk plots for the catecholase activity of MT assayed as oxidation of L-Dopa in the presence of different fixed concentrations of ligand

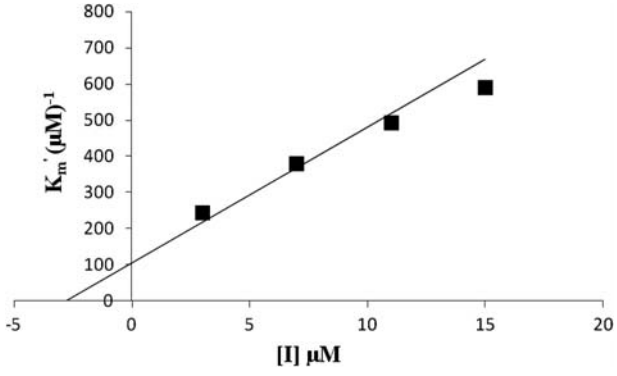

Figure 4. Secondary plot for the cresolase activity, the K_m' at given concentration of ligand vs. the concentration of ligand.

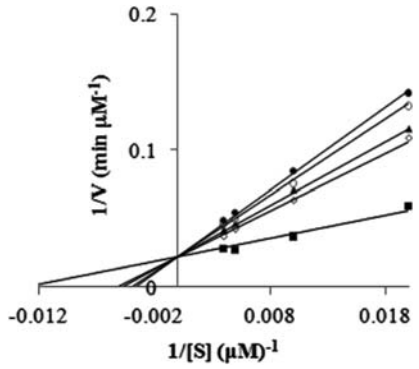

Figure 5. Double reciprocal Lineweaver-Burk plots of MT kinetic assay for catecholase reactions. L-Dopa was a substrate. The reaction was done in 10 mM sodium phosphate buffer, pH 6.8, at 20°C and 11.11 μg/ml enzyme, in the presence of different concentrations of ligand, 0 mM (■), 3 μM (◊), 4 μM (▲), 6 μM (◯), and 7 μM (●).

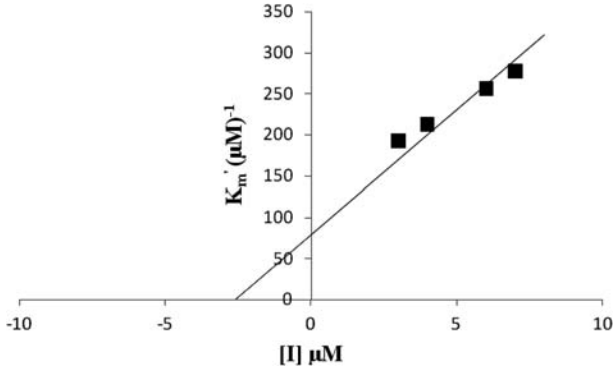

Figure 6. Secondary plot for the catecholase activity, the K_m' at given concentration of ligand vs. the concentration of ligand.

are shown in Figure 5. These plots give a set of straight lines intersecting exactly on the vertical axis. It is observed that the V_{max} value is unchanged by the inhibitor while the K_m' value is increased, revealing that the

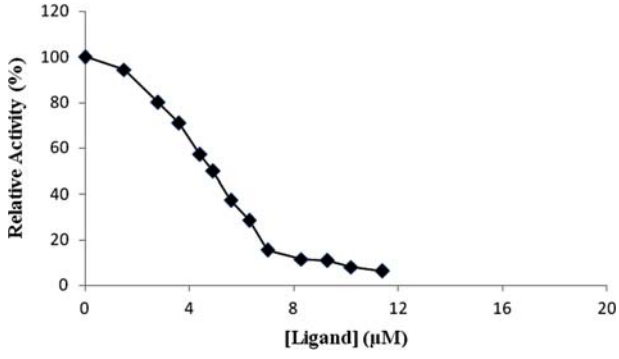

Figure 7. Plots of relative cresolase activity vs. [ligand]. The ligand concentrations are 0, 1.5, 2.8, 3.6, 4.4, 4.9, 5.6, 6.3, 7, 8.3, 9.3, 10.2, and 11.4 μM. The final L-tyrosine concentration was 150 μM.

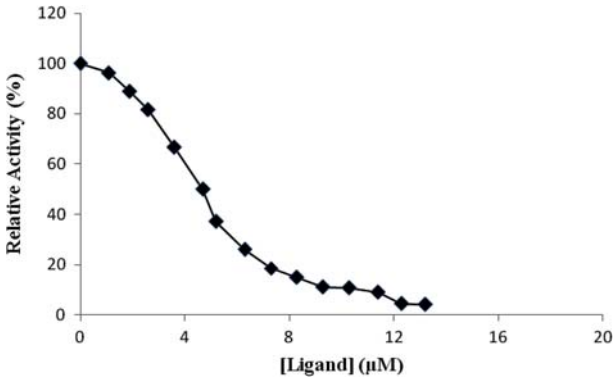

Figure 8. Plots of relative catecholase activity vs. [ligand]. The ligand concentrations are 0, 1.1, 1.9, 2.6, 3.6, 4.7, 5.2, 6.3, 7.3, 8.3, 9.3, 10.3, 11.4, 12.3, and 13.2 μM. The final L-tyrosine concentration was 100 μM.

ligand induces a competitive inhibition. Figure 6 shows the secondary plot, the K_m' value at a given concentration of ligand vs. the concentration of inhibitor, which gives the inhibition constants ($-K_i$) from the abscissa intercepts. The K_i value for ligand is 2.6 μM. The ligand binds to the substrate-binding site and inhibits the catecholase activity in the competitive mode. The small value of K_i for the ligand indicates that it tightly binds to the enzyme. The docking result not only shows the binding site of ligand, but also reveals the OH group of the ligand which has bound to the copper ion. Further, for calculating IC_{50}, the relative cresolase and catecholase activities of the MT against ligand concentration were plotted (Figures 7 and 8, respectively).

Ligand docking and molecular dynamics simulation

The results of docking the ligand with the enzyme are shown in Figure 9. As it is clear, the ligand is bound in the active site of MT and the OH group of the aromatic ring is bound to the copper ion.

The current ligand rough structure is depicted in Figure 10. R1 and R2 note for ring-like structure of ligand

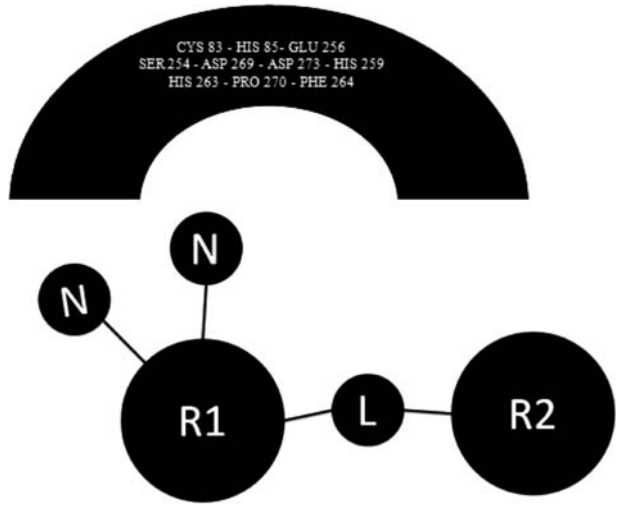

Figure 10. Schematic ligand rough structure. R1 and R2 note for ring-like structure of ligand molecule and L denotes the linker part. N notes for each nitro groups.

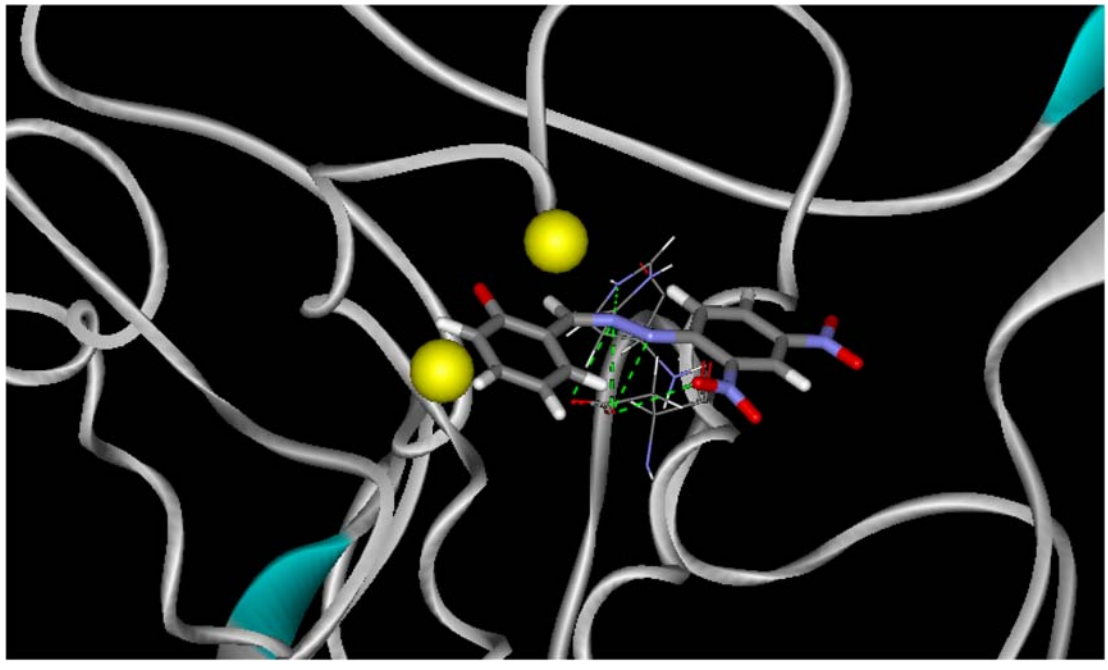

Figure 9. Computational docking results for tyrosinase and ligand. Yellow ones are copper ions of the active site and ligand is in stick and ball model and the histidine and aspartic residues are in line models.

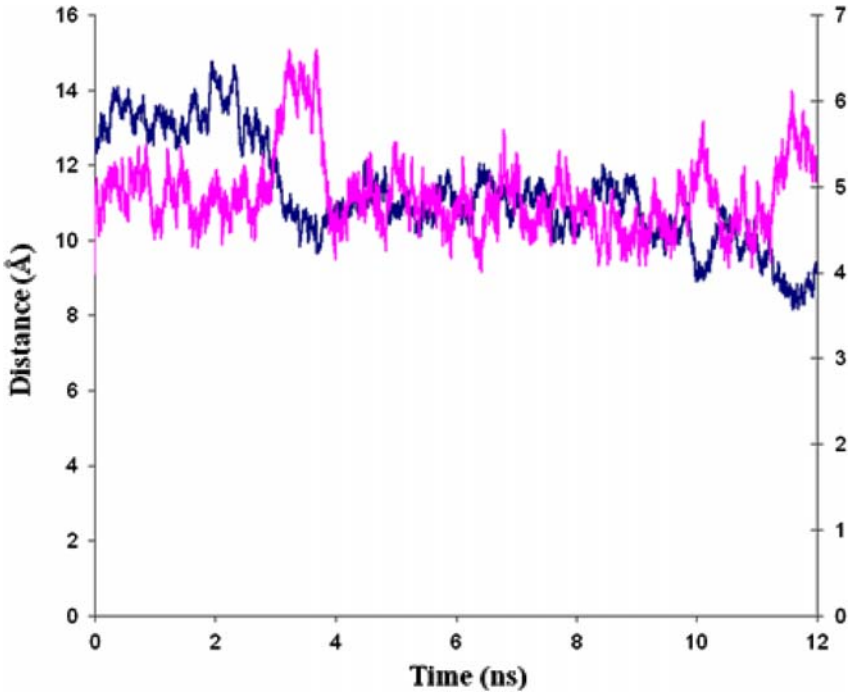

Figure 11. Molecular dynamics simulation between MT and ligand. The global ligand's structure distances from MT binding site acidic residues (pink line) and hydrophobic residues (blue line). Left and right *Y*-axes stand for distance from hydrophobic and acidic residues, respectively.

molecule, and L denotes the linker part. N notes for each nitro groups. The docking results indicate the position of ligand is stable and its neighbors are CYS 83, HIS 85, GLU 256, SER 254, ASP 269, ASP 273, HIS 259, HIS 263, PRO 270, and PHE 264, which are far from the ligand 5 Å at most.

The global ligand's structure distances from its binding site are shown in Figure 11. This is appeared that the

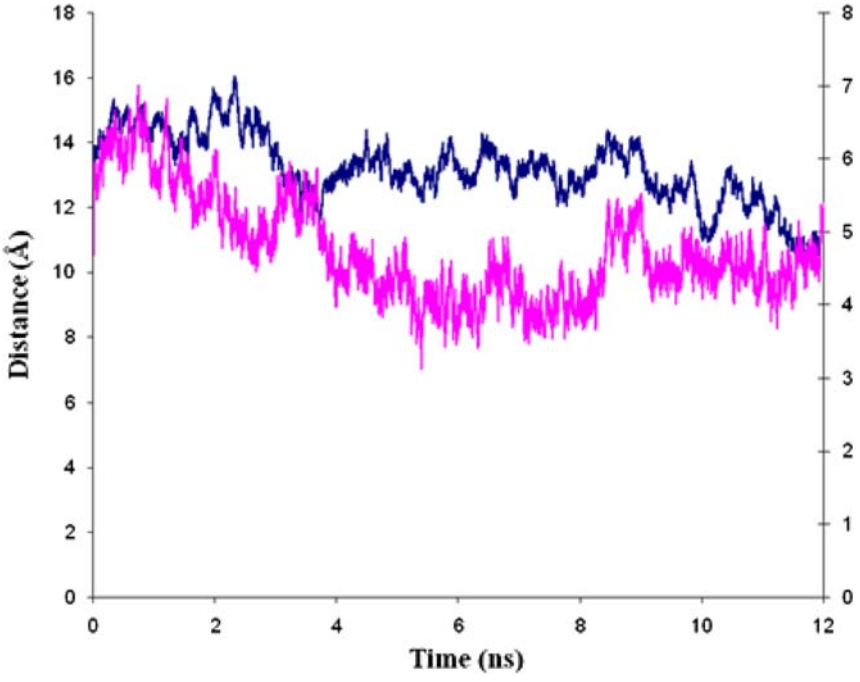

Figure 12. Molecular dynamics simulation between MT and ligand. The R1 distances from MT binding site acidic residues (pink line) and hydrophobic residues (blue line). Left and right *Y*-axes stand for distance from hydrophobic and acidic residues, respectively.

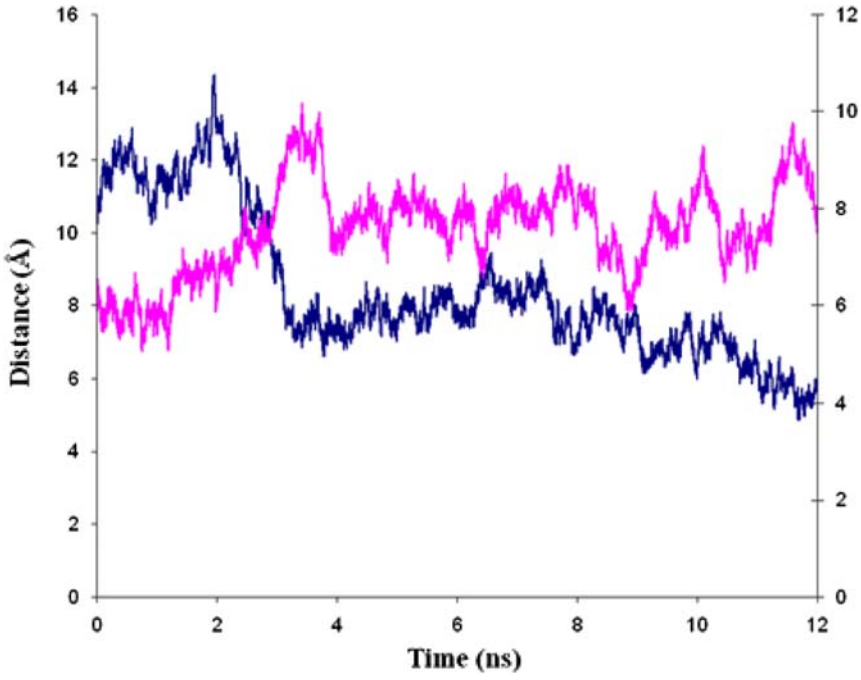

Figure 13. Molecular dynamics simulation between MT and ligand. The R2 distances from MT binding site acidic residues (pink line) and hydrophobic residues (blue line). Left and right *Y*-axes stand for distance from hydrophobic and acidic residues, respectively.

distance between ligand and hydrophobic parts of binding site decreases during MD and then it becomes constant. It indicates that the ligand is a hydrophobic molecule in which its binding site's hydrophobic interaction attracts it to the enzyme surface. The Global distance of ligand did not change from acidic residues of

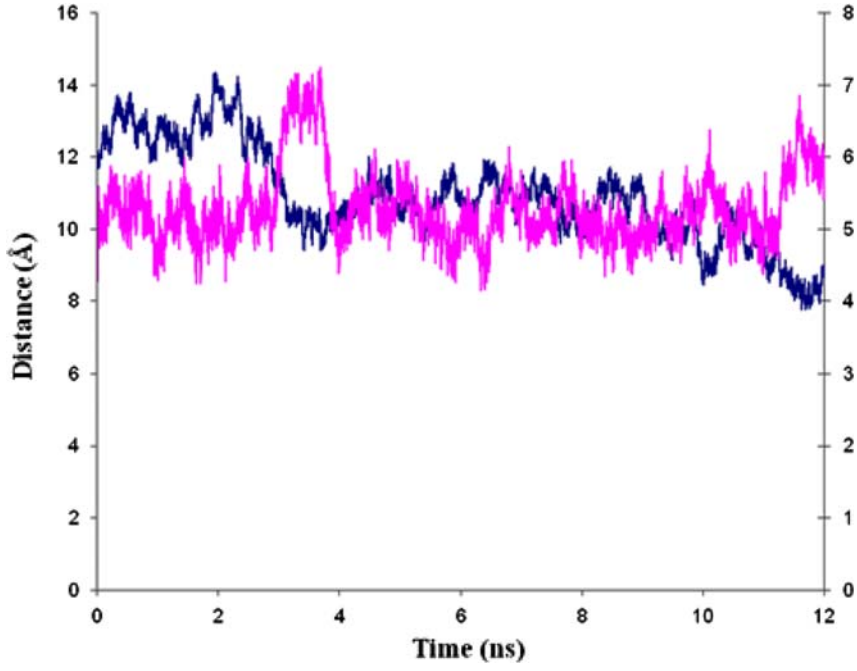

Figure 14. Molecular dynamics simulation between MT and ligand. The L distances from MT binding site acidic residues (pink line) and hydrophobic residues (blue line). Left and right *Y*-axes stand for distance from hydrophobic and acidic residues, respectively.

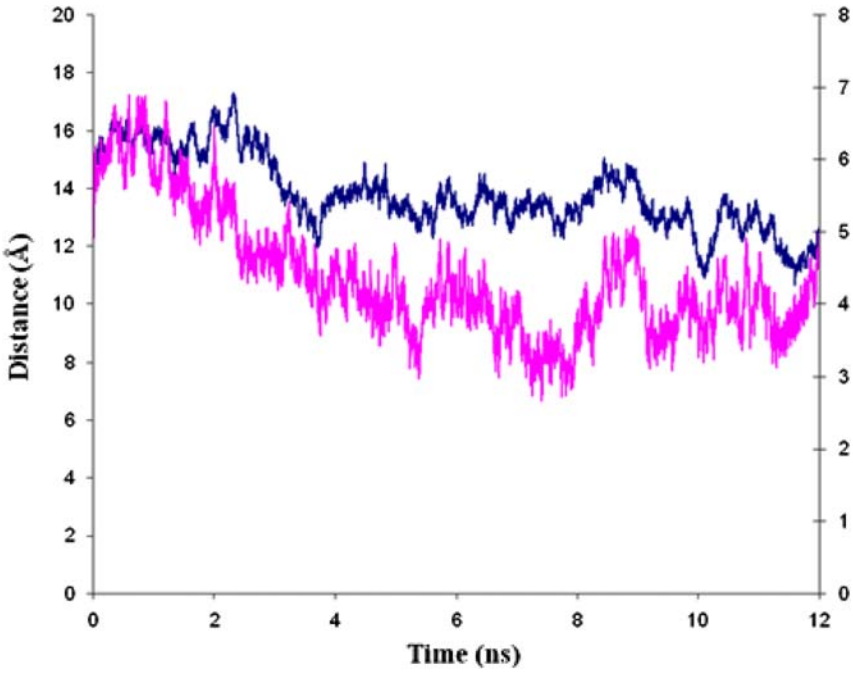

Figure 15. Molecular dynamics simulation between MT and ligand. The two hanging N parts of ligand distances from MT binding site acidic residues (pink line) and hydrophobic residues (blue line). Left and right *Y*-axes stand for distance from hydrophobic and acidic residues, respectively.

binding surface despite of a small rearrangement along the second to third nanosecond of simulation.

Figure 10 schemes the ligand in carton. More details of ligand binding mode were available upon ligand parts–binding surface distance studies. Figure 12 shows that the ligand ring 1 (R1) has a tendency toward acidic binding surface residues and it implies that this ring globally interacts with binding surface via electrostatic interactions. Figure 13 notes a fascinating result. There are hydrophobic interactions between ring 2 (R2) and binding surface because of the obvious R2–hydrophobic part of binding surface decreasing distance throughout MD.

The linker part (L) which contained two nitrogen atoms shows a pattern-like global distance from binding site (Figure 14). Two hanging N parts of ligand (as in Figure 10) clearly show an affinity toward acidic parts of binding surface (Figure 15).

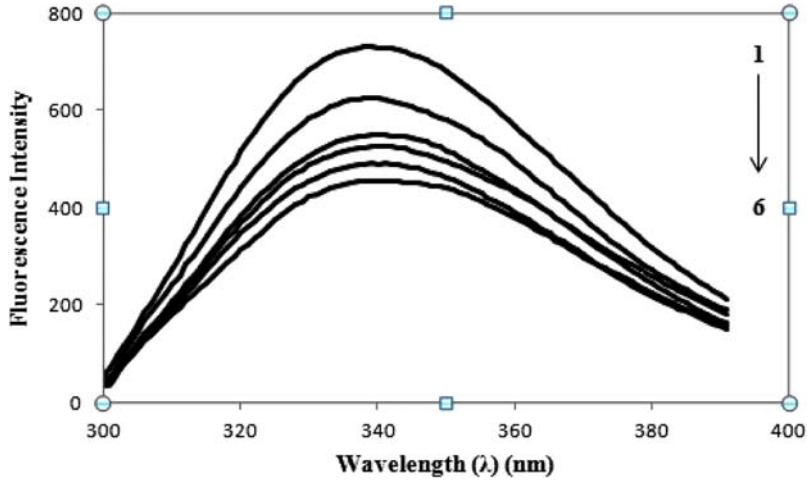

Figure 16. Emission spectra of tyrosinase at $\lambda_{max} = 290$ nm showing the quenching effect of increasing the concentration (2.7, 6, 7.5, 9.5, and 14 μM) of ligand.

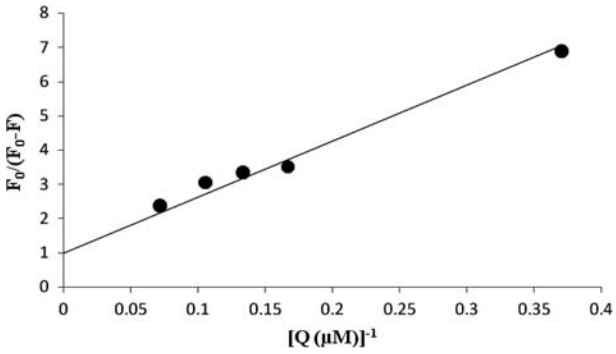

Figure 17. The secondary re-plot of $F_0/(F_0 - F)$ vs. $[Q]^{-1}$ according to Equation (1). Data were obtained from Figure 10 The final concentration of the enzyme was 1 μM.

Fluorescence quenching

Tryptophan fluorescence has been frequently examined among the intrinsic aromatic fluorophores in tyrosinase molecules to obtain information about conformational changes. The interaction of the ligand with tyrosinase and the conformational alterations in the enzyme were evaluated by measuring the intrinsic fluorescence intensities of the protein before and after the addition of the ligand. The fluorescence emission spectra of MT were collected at different concentrations of ligand. Figure 16 shows that the ligand causes a dramatic change in the fluorescence emission spectra.

In this study, the fluorescence intensities of the emission peaks were found to be inversely decreased by increasing the ligand concentration. Although the decline in the fluorescence intensity was caused due to quenching, there was no significant λ_{em} shift with the accumulation ligand.

A plot of the maximum fluorescence intensity vs. the concentration of the ligand revealed a linear relationship (Figure 17). From this data, we calculated the binding constant as $K = .061\ \mu M^{-1}$ and the binding number as $n = 1.02 \pm .6$ according to Equation (1). These results revealed that the newly synthesized ligand has a strong binding affinity for tyrosinase in the absence of substrate and that there is one possible binding site.

Discussion

The newly synthesized ligand competitively inhibited both the cresolase and catecholase activities of MT, with a small inhibition constant. The ligand competitively inhibited the enzyme by binding to its active site, which is also confirmed by docking results (Figure 9). The ligand could form a stable complex with copper ion and block the active site of MT and also make four hydrogen bonds with aspartic acid and one hydrogen bond with histidine residue in the active site. By comparing the K_i values of different inhibitors, it was found that the ligand is a powerful inhibitor (see Table 1).

Copper ions in the active site of MT play a major role in tyrosinase activity by catalyzing electron transfer to substrates. Formation of a complex between a ligand and the copper ion in the tyrosinase active site can prevent electron transfer by the metal ion, so that the enzyme cannot oxidize substrates and tyrosinase

Table 1. Comparing IC_{50} values of different inhibitors of MT (compounds with OH group) for both cresolase and catecholase activities.

Reaction type	Ligands	IC_{50} (μM)	References
Cresolase activity	2-((1Z)-(2-(2,4-dinitrophenyl)hydrazine-1-ylidene)methyl)phenol	4.9	–
Catecholase activity	2-((1Z)-(2-(2,4-dinitrophenyl)hydrazine-1-ylidene)methyl)phenol	4.7	–
	5-benzylidene(thio)barbiturate-b-D-glycosides	50	Yan et al. (2009)
	N-caffeoylserotonin	15.3	Yamazaki et al. (2009)
	N-protocatechuoylserotonin	111	Yamazaki (et al., 2009)
	N-cyclopentyl-*N*-nitrosohydroxylamine	.6	Shiino et al. (2001)
	Dopastin	20	Shiino et al. (2001)
	Neocupferron	46	Shiino et al. (2001)
	Sophoraflavone	6.6	Kim et al. (2003)
	Kuraridin	.6	Kim et al. (2003)
	Kurarinone	6.2	Kim et al. (2003)
	Artocarpanone	80.8	Arung et al. (2006)
	Kurarinol	8.6	Hyun et al. (2008)
	Kuraridinol	.8	Hyun et al. (2008)
	Trifulirhizin	506.77	Hyun et al. (2008)
	Oxyresveratrol	1	Shin et al. (1998)
	Resveratrol	155	Shin et al. (1998)
	3,5-Dihydroxy-4-methoxystilbene	252	Shin et al. (1998)
	3,4-Dimethoxy-5-hydroxystilbene	490	Shin et al. (1998)
	Trimethylresveratrol	500	Shin et al. (1998)

activity is inhibited. As Figure 9 shows, the synthesized ligand bound to the MT copper ion via an OH group further making four hydrogen bonds with the Asp and one hydrogen bond with the His residues in the active site. As it has been mentioned before, the histidine residues in the active site have an important role in the enzyme activity (Guo et al., 2008), so the ligand interrupted the MT activity by forming hydrogen bonds with it. Tyrosinase substrates (L-Dopa and L-tyrosine) also bind to the copper ion of tyrosinase via their OH group. However, the OH group of the new ligand is more acidic than the OH group of tyrosinase substrates, as its OH group was bound to an aromatic ring connected to an imine group. There is a resonance binding between two imine groups and the aromatic ring; therefore, it is expected that ionized OH group of the synthesized ligand is a powerful acidic group, which can bind to the copper ion of tyrosinase more strongly than other ligands. Tyrosinases have similar binuclear copper sites (Halaouli, Asther, Sigoillot, Hamdi, & Lomascolo, 2006), so MT can be used as a model for human tyrosinase and hence, we expect that human tyrosinase will also be competitively inhibited by our newly synthesized ligand.

At the end, from MD results, we conclude that this ligand binds to binding surface via electrostatic interaction that sourced in ring 1 (R1) and hydrophobic interactions which originated from ring 2 (R2). Figures 11–15 remind that the ligand never has gone far away from the binding site when compared with docking results structure. So, the binding mode seems good in this manner.

Acknowledgements

The financial support given by the University of Tehran is gratefully acknowledged.

References

Alijanianzadeh, M., Saboury, A.A., Mansuri-Torshizi, H., Haghbeen, K., & Moosavi-Movahedi, A.A. (2007). The inhibitory effect of some new synthesized xanthates on mushroom tyrosinase activities. *Journl of Enzyme Inhibition and Medicinal Chemistry, 22*, 239–246.

Amin, E., Saboury, A.A., Mansuri-Torshizi, H., & Moosavi-Movahedi, A.A. (2010). Potent inhibitory effects of benzyl and p-xylidine-bis dithiocarbamate sodium salts on activities of mushroom tyrosinase. *Journl of Enzyme Inhibition and Medicinal Chemistry, 25*, 272–281.

Artés, F.C., & Gil, M.I. (1998). Review: Enzymatic browning in minimally processed fruit and vegetables. *Journal of Agricultural and Food Chemistry, 4*, 377–389.

Arung, E.T., Shimizu, K., & Kondo, R. (2006). Inhibitory effect of artocarpanone from *Artocarpus heterophyllus* on melanin biosynthesis. *Biological & Pharmaceutical Bulletin, 29*, 1966–1969.

Banappagari, S., Ronald, S., & Satyanarayanajois, S.D. (2010). A conformationally constrained peptidomimetic binds to the extracellular region of HER2 protein. *Journal of Biomolecular Structure and Dynamics, 28*, 289–308.

Cabanes, J., Garcia-Canovas, F., Lozano, J.A., & Garcia-Carmona, F. (1987). A kinetic study of the melanization pathway between L-tyrosine and dopachrome. *Biochimica et Biophysica Acta, 923*, 187–195.

Cambria, M.T., Di Marino, D., Falconi, M., Garavaglia, S., & Cambria, A. (2010). Docking simulation and competitive experiments validate the interaction between the 2,5-xylidine inhibitor and *Rigidoporus lignosus* laccase. *Journal of Biomolecular Structure and Dynamics, 27*, 501–510.

Chang, T.T., Huang, H.J., Lee, K.J., Yu, H.W., Chen, H.Y., Tsai, F.J., … Chen, C.Y. (2010). Key features for designing phosphodiesterase-5 inhibitors. *Journal of Biomolecular Structure and Dynamics, 28*, 309–321.

Chen, Q.X., & Kubo, I. (2002). Kinetics of mushroom tyrosinase inhibition by quercetin. *Journal of Agricultural and Food Chemistry, 50*, 4108–4112.

Cho, I.H., Lu, Z.R., Yu, J.R., Park, Y.D., Yang, J.M., Hahn, M. J., & Zou, F. (2009). Towards profiling the gene expression of tyrosinase-induced melanogenesis in HEK293 cells: A functional DNA chip microarray and interactomics studies. *Journal of Biomolecular Structure and Dynamics, 27*, 331–346.

Cooksey, C.J., Garratt, P.J., Land, E.J., Pavel, S., Ramsden, C. A., Riley, P.A., & Smit, N.P. (1997). Evidence of the indirect formation of the catecholic intermediate substrate responsible for the autoactivation kinetics of tyrosinase. *Journal of Biological Chemistry, 272*, 26226–26235.

Cooksey, C.J., Garratt, P.J., Land, E.J., Ramsden, C.A., & Riley, P.A. (1998). Tyrosinase kinetics: Failure of the autoactivation mechanism of monohydric phenol oxidation by rapid formation of a quinomethane intermediate. *Biochemical Journal, 333*, 685–691.

da Cunha, E.E., Barbosa, E.F., Oliveira, A.A., & Ramalho, T.C. (2010). Molecular modeling of Mycobacterium tuberculosis DNA gyrase and its molecular docking study with gatifloxacin inhibitors. *Journal of Biomolecular Structure and Dynamics, 27*, 619–625.

Eicken, C., Krebs, B., & Sacchettini, J.C. (1999). Catechol oxidase – structure and activity. *Current Opinion in Structural Biology, 9*, 677–683.

Fu, B., Li, H., Wang, X., Lee, F.S., & Cui, S. (2005). Isolation and identification of flavonoids in licorice and a study of their inhibitory effects on tyrosinase. *Journal of Agricultural and Food Chemistry, 53*, 7408–7414.

Gao, H., Nishida, J., Saito, S., & Kawabata, J. (2007). Inhibitory effects of 5,6,7-trihydroxyflavones on tyrosinase. *Molecules, 12*, 86–97.

Gheibi, N., Saboury, A.A., Haghbeen, K., & Moosavi-Movahedi, A.A. (2005). Activity and structural changes of mushroom tyrosinase induced by *n*-alkyl sulfates. *Colloids and Surfaces B Biointerfaces, 45*, 104–107.

Gheibi, N., Saboury, A.A., Mansuri-Torshizi, H., Haghbeen, K., & Moosavi-Movahedi, A.A. (2005). The inhibition effect of some *n*-alkyl dithiocarbamates on mushroom tyrosinase. *Journal of Enzyme Inhibition and Medicinal Chemistry, 20*, 393–399.

Guo, L., Lu, Z.R., Park, D., Oh, S.H., Shi, L., Park, S.J., … Zou, F. (2008). The effect of histidine residue modification on tyrosinase activity and conformation: Inhibition kinetics and computational prediction. *Journal of Biomolecular Structure and Dynamics, 26*, 395–402.

Haghbeen, K., Saboury, A.A., & Karbassi, F. (2004). Substrate share in the suicide inactivation of mushroom tyrosinase. *Biochimica et Biophysica Acta, 1675*, 139–146.

Halaban, R., Patton, R.S., Cheng, E., Svedine, S., Trombetta, E.S., Wahl, M.L., … Hebert, D.N. (2002). Abnormal acidification of melanoma cells induces tyrosinase retention in the early secretory pathway. *Journal of Biological Chemistry, 277*, 14821–14828.

Halaouli, S., Asther, M., Sigoillot, J.C., Hamdi, M., & Lomascolo, A. (2006). Fungal tyrosinases: New prospects in molecular characteristics, bioengineering and biotechnological applications. *Journal of Applied Microbiology, 100*, 219–232.

Han, H.Y., Lee, J.R., Xu, W.A., Hahn, M.J., Yang, J.M., & Park, Y.D. (2007). Effect of Cl^- on tyrosinase: Complex inhibition kinetics and biochemical implication. *Journal of Biomolecular Structure and Dynamics, 25*, 165–171.

Huang, H.J., Lee, K.J., Yu, H.W., Chen, H.Y., Tsai, F.J., & Chen, C.Y. (2010). A novel strategy for designing the selective PPAR agonist by the 'sum of activity' model. *Journal of Biomolecular Structure and Dynamics, 28*, 187–200.

Hyun, S.K., Lee, W.H., Jeong da, M., Kim, Y., & Choi, J.S. (2008). Inhibitory effects of kurarinol, kuraridinol, and trifolirhizin from *Sophora flavescens* on tyrosinase and melanin synthesis. *Biological & Pharmaceutical Bulletin, 31*, 154–158.

Ismaya, W.T., Rozeboom, H.J., Schurink, M., Boeriu, C.G., Wichers, H., & Dijkstra, B.W. (2011). Crystallization and preliminary X-ray crystallographic analysis of tyrosinase from the mushroom *Agaricus bisporus*. *Acta Crystallographica Section F: Structural Biology and Crystallization Communications, 67*, 575–578.

Ismaya, W.T., Rozeboom, H.J., Weijn, A., Mes, J.J., Fusetti, F., Wichers, H.J., & Dijkstra, B.W. (2011). Crystal structure of *Agaricus bisporus* mushroom tyrosinase: Identity of the tetramer subunits and interaction with tropolone. *Biochemistry, 50*, 5477–5486.

Jeong, S.H., Ryu, Y.B., Curtis-Long, M.J., Ryu, H.W., Baek, Y. S., Kang, J.E., & Park, K.H. (2009). Tyrosinase inhibitory polyphenols from roots of *Morus lhou*. *Journal of Agricultural and Food Chemistry, 57*, 1195–1203.

Kahlon, A.K., Roy, S., & Sharma, A. (2010). Molecular docking studies to map the binding site of squalene synthase inhibitors on dehydrosqualene synthase of *Staphylococcus aureus*. *Journal of Biomolecular Structure and Dynamics, 28*, 201–210.

Kanade, S.R., Suhas, V.L., Chandra, N., & Gowda, L.R. (2007). Functional interaction of diphenols with polyphenol oxidase. Molecular determinants of substrate/inhibitor specificity. *FEBS Journal, 274*, 4177–4187.

Karbassi, F.H., Saboury, A.A., Ranjbar, B., & Moosavi-Movahedi, A.A. (2003). Activity, structural and stability changes of mushroom tyrosinase by sodium dodecyl sulfate. *Colloids and Surfaces B: Biointerfaces, 32*, 137–143.

Kim, D., Park, J., Kim, J., Han, C., Yoon, J., Kim, N., … Lee, C. (2006). Flavonoids as mushroom tyrosinase inhibitors: A fluorescence quenching study. *Journal of Agricultural and Food Chemistry, 54*, 935–941.

Kim, S.J., Son, K.H., Chang, H.W., Kang, S.S., & Kim, H.P. (2003). Tyrosinase inhibitory prenylated flavonoids from *Sophora flavescens*. *Biological & Pharmaceutical Bulletin, 26*, 1348–1350.

Kubo, I., & Kinst-Hori, I. (1999). Flavonols from saffron flower: Tyrosinase inhibitory activity and inhibition mechanism. *Journal of Agricultural and Food Chemistry, 47*, 4121–4125.

Kubo, I., Kinst-Hori, I., Chaudhuri, S.K., Kubo, Y., Sanchez, Y., & Ogura, T. (2000). Flavonols from *Heterotheca inuloides*: Tyrosinase inhibitory activity and structural criteria. *Bioorganic & Medicinal Chemistry, 8*, 1749–1755.

Lee, S.H., Choi, S.Y., Kim, H., Hwang, J.S., Lee, B.G., Gao, J. J., & Kim, S.Y. (2002). Mulberroside F isolated from the leaves of *Morus alba* inhibits melanin biosynthesis. *Biological & Pharmaceutical Bulletin, 25*, 1045–1048.

Mason, H.S. (1948). The chemistry of melanin: III. Mechanism of the oxidation of dihydroxyphenylalanine by tyrosinase. *Journal of Biological Chemistry, 172*, 83–99.

Nasiri, R., Bahrami, H., Zahedi, M., Moosavi-Movahedi, A.A., & Sattarahmady, N. (2010). A theoretical elucidation of glucose interaction with HSA's domains. *Journal of Biomolecular Structure and Dynamics, 28*, 211–226.

Nekrasov, A.N., & Zinchenko, A.A. (2010). Structural features of the interfaces in enzyme-inhibitor complexes. *Journal of Biomolecular Structure and Dynamics, 28*, 85–96.

Ompraba, G., Velmurugan, D., Louis, P.A., & Rafi, Z.A. (2010). Molecular modeling of the additional inhibitor site located in secretory phospholipase A(2). *Journal of Biomolecular Structure and Dynamics, 27*, 489–500.

Orlow, S.J., Zhou, B.K., Chakraborty, A.K., Drucker, M., Pifko-Hirst, S., & Pawelek, J.M. (1994). High-molecular-weight forms of tyrosinase and the tyrosinase-related proteins: Evidence for a melanogenic complex. *Journal of Investigative Dermatology, 103*, 196–201.

Park, Y.D., Lyou, Y.J., Hahn, H.S., Hahn, M.J., & Yang, J.M. (2006). Complex inhibition of tyrosinase by thiol-composed Cu^{2+} chelators: A clue for designing whitening agents. *Journal of Biomolecular Structure and Dynamics, 24*, 131–138.

Parvez, S., Kang, M., Chung, H.S., & Bae, H. (2007). Naturally occurring tyrosinase inhibitors: Mechanism and applications in skin health, cosmetics and agriculture industries. *Phytotherapy Research, 21*, 805–816.

Phillips, J.C., Braun, R., Wang, W., Gumbart, J., Tajkhorshid, E., Villa, E., … Schulten, K. (2005). Scalable molecular dynamics with NAMD. *Journal of Computational Chemistry, 26*, 1781–1802.

Prezioso, J.A., Epperly, M.W., Wang, N., & Bloomer, W.D. (1992). Effects of tyrosinase activity on the cytotoxicity of 4-S-cysteaminylphenol and *N*-acetyl-4-S-cysteaminylphenol in melanoma cells. *Cancer Letters, 63*, 73–79.

Ramalho, T.C., Rocha, M.V., da Cunha, E.F., Oliveira, L.C., & Carvalho, K.T. (2010). Understanding the molecular behavior of organotin compounds to design their effective use as agrochemicals: Exploration via quantum chemistry and experiments. *Journal of Biomolecular Structure and Dynamics, 28*, 227–238.

Raper, H.S. (1928). The aerobic oxidases. *Physiology Review, 8*, 245–282.

Rescigno, A., Sollai, F., Pisu, B., Rinaldi, A., & Sanjust, E. (2002). Tyrosinase inhibition: General and applied aspects. *Journal of Enzyme Inhibition and Medicinal Chemistry, 17*, 207–218.

Ritchie, D.W. (2003). Evaluation of protein docking predictions using Hex 3.1 in CAPRI rounds 1 and 2. *Proteins, 52*, 98–106.

Robb, D.A. (1984). Tyrosinase. In R. Lontie (Ed.), *Copper proteins and copper enzymes* (Vol. II, pp. 207–240). Boca Raton, FL: CRC Press.

Saboury, A.A., & Alijanianzadeh, M. (2008). Ethyl xanthate and propyl xanthate as activators and inhibitors of mushroom tyrosinase in different concentrations. *Journal of Chinese Chemical Society, 55*, 937–942.

Saboury, A.A., Alijanianzadeh, M., & Mansoori-Torshizi, H. (2007). The role of alkyl chain length in the inhibitory effect *n*-alkyl xanthates on mushroom tyrosinase activities. *Acta Biochimica Polonica, 54*, 183–191.

Saboury, A.A., Karbassi, F., Haghbeen, K., Ranjbar, B., Moosavi-Movahedi, A.A., & Farzami, B. (2004). Stability, structural and suicide inactivation changes of mushroom tyrosinase after acetylation by N-acetylimidazole. *International Journal of Biological Macromolecules, 34*, 257–262.

Sanchez-Ferrer, A., Rodriguez-Lopez, J.N., Garcia-Canovas, F., & Garcia-Carmona, F. (1995). Tyrosinase: A comprehensive review of its mechanism. *Biochimica et Biophysica Acta, 1247*, 1–11.

Schallreuter, K.U.K, Kothari, S., Chavan, B., & Spencer, J.D. (2008). Regulation of melanogenesis–controversies and new concepts. *Experimental Dermatology, 17*, 395–404.

Shareefi Borojerdi, S., Haghbeen, K., Asghar Karkhane, A., Fazli, M., & Saboury, A.A. (2004). Successful resonance Raman study of cresolase activity of mushroom tyrosinase. *Biochemical and Biophysical Research Communication, 314*, 925–930.

Shiino, M., Watanabe, Y., & Umezawa, K. (2001). Synthesis of N-substituted N-nitrosohydroxylamines as inhibitors of mushroom tyrosinase. *Bioorganic & Medicinal Chemistry, 9*, 1233–1240.

Shiino, M., Watanabe, Y., & Umezawa, K. (2003). Synthesis and tyrosinase inhibitory activity of novel N-hydroxybenzyl-N-nitrosohydroxylamines. *Bioorganic Chemistry, 31*, 129–135.

Shimizu, K., Kondo, R., & Sakai, K. (2000). Inhibition of tyrosinase by flavonoids, stilbenes and related 4-substituted resorcinols: Structure–activity investigations. *Planta Medica, 66*, 11–15.

Shin, N.H., Ryu, S.Y., Choi, E.J., Kang, S.H., Chang, I.M., Min, K.R., & Kim, Y. (1998). Oxyresveratrol as the potent inhibitor on dopa oxidase activity of mushroom tyrosinase. *Biochemical and Biophysical Research Communication, 243*, 801–803.

Si, Y.X., Yin, S.J., Park, D., Chung, H.Y., Yan, L., Lu, Z.R., … Park, Y.D. (2011). Tyrosinase inhibition by isophthalic acid: Kinetics and computational simulation. *International Journal of Biological Macromolecules, 48*, 700–704.

Tao, Y., Rao, Z.H., & Liu, S.Q. (2010). Insight derived from molecular dynamics simulation into substrate-induced changes in protein motions of proteinase K. *Journal of Biomolecular Structure and Dynamics, 28*, 143–158.

Whitaker, J.R. (1995). Polyphenoloxidas. In D.W.S. Wong (Ed.), *Food enzymes, structure and mechanism* (pp. 271–307). New York, NY: Chapman & Hall.

Xie, M.X., Xu, X.Y., & Wang, Y.D. (2005). Interaction between hesperetin and human serum albumin revealed by spectroscopic methods. *Biochimica et Biophysica Acta, 1724*, 215–224.

Yamazaki, Y., Kawano, Y., Yamanaka, A., & Maruyama, S. (2009). N-[(Dihydroxyphenyl)acyl]serotonins as potent inhibitors of tyrosinase from mouse and human melanoma cells. *Bioorganic & Medicinal Chemistry Leters, 19*, 4178–4182.

Yan, Q., Cao, R., Yi, W., Yu, L., Chen, Z., Ma, L., & Song, H. (2009). Synthesis and evaluation of 5-benzylidene(thio)barbiturate-beta-D-glycosides as mushroom tyrosinase inhibitors. *Bioorganic & Medicinal Chemistry Letters, 19*, 4055–4058.

Yang, Z., Wu, N., Fu, Y., Yang, G., Wang, W., Zu, Y., & Efferth, T. (2010). Anti-infectious bronchitis virus (IBV) activity of 1,8-cineole: Effect on nucleocapsid (N) protein. *Journal of Biomolecular Structure and Dynamics, 28*, 323–330.

Yin, S.J., Si, Y.X., Wang, Z.J., Wang, S.F., Oh, S., Lee, S., … Park, Y.D. (2011). The effect of thiobarbituric acid on tyrosinase: Inhibition kinetics and computational simulation. *Journal of Biomolecular Structure and Dynamics, 29*, 463–470.

Yokota, T., Nishio, H., Kubota, Y., & Mizoguchi, M. (1998). The inhibitory effect of glabridin from licorice extracts on melanogenesis and inflammation. *Pigment Cell Research, 11*, 355–361.

Zawistowski, J., Biliaderis, C.G., & Eskin, N.A.M. (1991). Polyphenol oxidase. In D.S.E. Robonson & N.A.M. Eskin (Eds.), *Oxidative enzymes in foods* (pp. 217–273). London: Elsevier.